ELSEVIER

Synthesis, structure, optical properties, and electronic structure of NaLiCdS$_2$

Bin Deng[a], George H. Chan[a], Fu Qiang Huang[b], Danielle L. Gray[a], Donald E. Ellis[a,c], Richard P. Van Duyne[a], James A. Ibers[a,*]

[a]Department of Chemistry, Northwestern University, 2145 Sheridan Road, Evanston, IL 60208-3113, USA
[b]Shanghai Institute of Ceramics, 1295 Dingxi Road, Shanghai 200050, PR China
[c]Department of Physics and Astronomy, Northwestern University, 2145 Sheridan Road, Evanston, IL 60208-3113, USA

Abstract

The new compound NaLiCdS$_2$ has been synthesized by the reaction of Cd and a Li$_2$S/S/Na$_2$S flux at 773 K. This compound, which has the Ce$_2$O$_2$S structure type, crystallizes with one formula unit in space group $P\bar{3}m1$ of the trigonal system in a cell at $T = 153$ K with $a = 4.1320(3)$ Å and $c = 6.8666(11)$ Å. The structure consists of two-dimensional $^2_\infty$[LiCdS$_2$] layers stacked perpendicular to the [001] direction. The two-dimensional layers are formed by corner-sharing LiS$_4$ or CdS$_4$ tetrahedra. The Na atoms are between these layers. Li incorporation in the compound is confirmed by an SIMS chemical composition map and by ICP measurements. The Li and Cd atoms are disordered in the crystal structure. First-principles calculations show that the optical excitations arise primarily from S→Cd charge-transfer transitions at 1.0 eV (very weak) and 2.4 eV (strong). Calculations also indicate that Na contributions around the Fermi level are significant. Polarized single-crystal optical measurements indicate an indirect optical band gap of 2.37 eV for light perpendicular to the (001) crystal face, in good agreement with theory. The compound NaLiZnS$_2$ has also been synthesized and is found to be isostructural with NaLiCdS$_2$.
© 2006 Elsevier Inc. All rights reserved.

Keywords: Quaternary Li-containing sulfides; Syntheses; Crystal structures; Electronic structures; Band gaps

1. Introduction

Many ternary and quaternary alkali-metal chalcogenides have been synthesized [1], mainly by the reactive flux method [2]. Most of these contain the heavier alkali metals Cs, Rb, or K. Although it is more difficult to obtain chalcogenides containing the lighter alkali metals Na or Li by this method some have been synthesized. Examples include LiAuS [3], Li$_3$AuS$_2$ [3], Li$_4$GeS$_4$ [4], Li$_{0.5}$Pb$_{1.75}$GeS$_4$ [5], LiEuPSe$_4$ [6], Li$_2$PbGeS$_4$ [7], Li$_2$EuGeS$_4$ [7], Na$_8$Pb$_2$Ge$_4$S$_{12}$ [8], Na$_6$Pb$_3$(PS$_4$)$_4$ [9], Na$_{1.5}$Pb$_{1.75}$GeS$_4$ [5], and Na$_{1.5}$Pb$_{0.75}$GeS$_4$ [5].

More recently, the reactive flux method was extended to the synthesis of mixed alkali-metal chalcogenides. Thus, the six new Li-containing compounds K$_2$LiVS$_4$, Rb$_2$LiVS$_4$, Cs$_2$LiVS$_4$, Rb$_2$LiNbS$_4$, Cs$_2$LiNbS$_4$, and Rb$_2$LiTaS$_4$ were synthesized in Li$_2$S/S/A_2S$_3$ (A = K, Rb, Cs) fluxes [10]. These Li$_2$S/A_2S$_3$ fluxes were observed to have even lower melting points than A_2S$_3$ fluxes and thus are suitable for the facile incorporation of the lighter alkali metals. Here, we show that Li$_2$S/S/Na$_2$S fluxes may also be used successfully. We report the synthesis of NaLiCdS$_2$, together with details on its crystal structure, optical properties, and electronic structure. The synthesis of the isostructural compound NaLiZnS$_2$ is also reported.

2. Experiment section

2.1. Syntheses of NaLiCdS$_2$ and NaLiZnS$_2$

The following reactants were used as obtained: Na$_2$S powder (Reacton, 99.9%), Li metal rods (Reacton, 99.9%), Cd powder (Aldrich, 99.9%), Zn powder (Strem, 99.9%), S

(Alfa, 99.9%), and Li_2S (Aldrich, 98%). For the syntheses of $NaLiCdS_2$ and $NaLiZnS_2$ reaction mixtures of 1.0 mmol Na_2S, 2.0 mmol of M (M = Cd, Zn), 1.0 mmol of Li_2S, and 2.0 mmol of S were loaded into fused-silica tubes under an Ar atmosphere in a glove box. These tubes were evacuated to about 10^{-4} Torr, sealed, and placed in a computer-controlled furnace. The samples were heated to 773 K in 5 h, kept at 773 K for 3 days, and then cooled at 3 K/h to 298 K. The products were washed with de-ionized water and dried with methanol. The presence of Na, Cd or Zn, and S in these compounds was confirmed by EDX analysis with the use of a Hitachi S-3500 SEM. These compounds are stable in air for several weeks.

2.2. Analysis of $NaLiCdS_2$

The chemical composition map of $NaLiCdS_2$ was taken by SIMS (TRIFT III ToF-SIMS) with the use of 15 keV Ga ions as the primary ions. Positive Na, Li, Cd, and negative S secondary ions were used to form the images of a selected crystal. The images were taken with an area of 240 µm × 240 µm (Fig. 1). These maps confirm the presence of Li but do not quantify it. To determine the Cd:Li and Li:Na ratios, 3.2 mg of $NaLiCdS_2$ crystals were dissolved in 10 mL of a 3% acid solution of Omni Trace HNO_3 in ultra pure water. The solution was then further diluted to 1 mL in 10 and to 1 mL in 3 to bring the concentrations of Cd and Na, respectively, within the limits of a Varian VISTA-MPX ICP instrument. Four standards each for Li, Cd, and Na were used to calibrate the instrument. Found were Cd:Li = 1.06(1):1; Li:Na = 0.99(2):1.
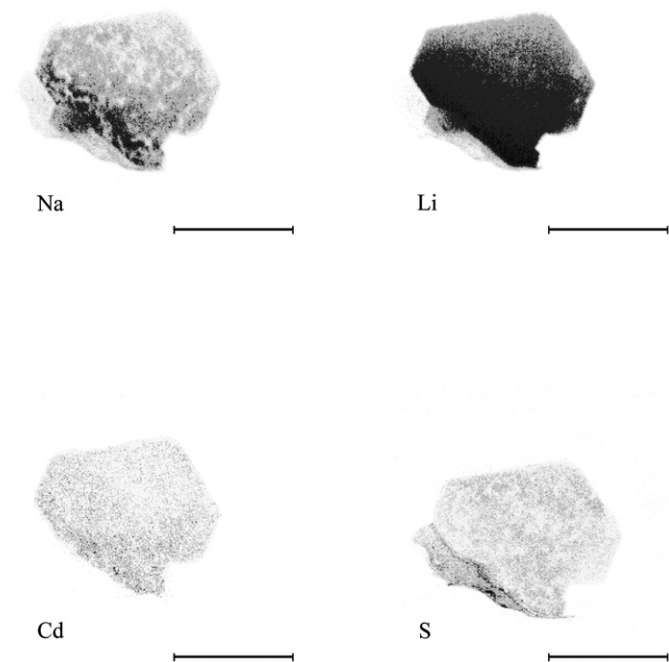

Fig. 1. The chemical composition maps of $NaLiCdS_2$ (scale bar is 100 µm).

2.3. Structure determinations

Single crystal X-ray diffraction data for $NaLiCdS_2$ and $NaLiZnS_2$ were collected with the use of graphite-mono-chromatized Mo$K\alpha$ radiation ($\lambda = 0.71073$ Å) at 153 K on a Bruker Smart-1000 CCD diffractometer [11]. The crystal-to-detector distance was 5.023 cm. Crystal decay was monitored by re-collecting 50 initial frames at the end of data collection. Data were collected by a scan of $0.3°$ in ω in groups of 606 frames for each of the φ settings $0°$, $90°$, $180°$, and $270°$. The collections of the intensity data were carried out with the program SMART [11]. The exposure time was 15 s/frame. Cell refinement and data reduction were carried out with the use of the program SAINT [11] and face-indexed absorption corrections were performed numerically with the use of the program XPREP [12]. Then the program SADABS [11] was employed to make incident beam and decay corrections.

The positions of the Na, Cd, and S atoms of $NaLiCdS_2$ in space group $P\bar{3}m1$ were found with the use of the direct-methods program SHELXS [12]. There is one formula unit in the cell; the Na atom is at the $1a$ position $(0,0,0)$, the S atoms are at $2d$ positions $\pm(1/3,2/3,z)$, and the Cd atoms are at $2d$ positions at half occupancy. With the use of the least-squares program SHELXL [12] this solution refined nicely. The ensuing difference electron density map was featureless. The structure comprises Na octahedrally coordinated by six S atoms and Cd tetrahedrally coordinated by four S atoms. In sulfides Li is often four-coordinate, for example in ALiS (A = Na, K) [13], $KLiMS_2$ (M = Mn, Zn) [14], and $LiGaS_2$ [15,16]. Because Cd:Li = 1.06(1):1 from the ICP results and because Cd^{2+} and Li^{1+} have similar crystal radii [17] of 0.92 and 0.73 Å, respectively, it is reasonable to assume that the Cd and Li atoms share equally the same $2d$ positions. In this way charge balance is achieved with the formal oxidation states $Na^+Li^+Cd^{2+}S^{2-}$. Given the small X-ray scattering power of Li compared to Cd, detection of the presumed Li position in the vicinity of the Cd position is not possible. Accordingly, the Li coordinates, displacement parameters, and occupancy were made equal to those of Cd. A refinement in which the (Cd/Li) occupancy was varied led to a value of 0.994, which was set equal to 1.00 in the final refinement. The program STRUCTURE TIDY [18] was then employed to standardize the atomic coordinates. The structure of $NaLiZnS_2$ was refined similarly. Additional experimental details are shown in Table 1 and in Supporting information. Selected metrical details are given in Table 2.

2.4. Single-crystal absorption measurement of $NaLiCdS_2$

A selected single crystal of $NaLiCdS_2$ was face-indexed, and its dimensions were measured by means of the video attachment of a Bruker Smart-1000 CCD diffractometer. Optical measurements were performed with the use of an Ocean Optics model S2000 spectrometer coupled fiber-

Table 1
Crystal data and structure refinements for NaLiMS$_2$ (M = Cd, Zn)[a]

	NaLiCdS$_2$	NaLiZnS$_2$
Formula weight	206.45	159.42
Space group	$P\bar{3}m1$	$P\bar{3}m1$
a (Å)	4.1320(3)	3.9711(3)
c (Å)	6.8666(11)	6.7186(12)
V (Å^3)	101.530(19)	91.755(19)
Z	1	1
ρ_c (g/cm^3)	3.377	2.885
μ (cm^{-1})	62.66	76.75
$R(F)$[b]	0.0139	0.0229
$R_w(F_o^2)$[c]	0.0329	0.0684

[a] For both structures $T = 153(2)$ K and $\lambda = 0.71073$ Å.
[b] $R(F) = \Sigma||F_o| - |F_c||/\Sigma|F_o|$ for $F_o^2 > 2\sigma(F_o^2)$.
[c] $R_w(F_o^2) = \{\Sigma[w(F_o^2 - F_c^2)^2]/\Sigma wF_o^4\}^{1/2}$ for all data. $w^{-1} = \sigma^2(F_o^2) + (qF_o^2)^2$ where $q = 0.02$ for NaLiCdS$_2$ and 0.04 for NaLiZnS$_2$.

Table 2
Selected distances (Å) and angles (deg)

	NaLiCdS$_2$	NaLiZnS$_2$
Na–S × 6	2.9590(3)	2.9100(5)
M–S × 3	2.5039(2)	2.3987(3)
M–S	2.6051(7)	2.429(1)
S–Na–S	88.57(1)	86.05(2)
S–M–S	111.20(1)	111.74(2)
S–M–S	107.68(1)	107.09(2)

optically to a Nikon TE300 inverted microscope over the range 400 nm (3.10 eV) to 800 nm (1.55 eV) at 293 K. The plate-like single crystal with dimensions of 62, 174, 160, and 146 μm along [001], [100], [010], and [$\bar{1}$10], respectively, was mounted on a glass fiber, and positioned at the focal point above a 20 × objective with the use of a goniometer mounted on a translation stage (Line Tool Company). Fine alignment of the microscope assembly was achieved by maximizing the transmission of the lamp profile. Polarized light (tungsten-halogen lamp) transmitted through the crystal was then spatially filtered before being focused into the 400 μm core diameter fiber coupled to the spectrometer. The absorbance spectrum of light perpendicular to the (001) crystal face of NaLiCdS$_2$ was collected.

2.5. Electronic structure calculations for NaLiCdS$_2$

The Li and Cd atoms are disordered equally on $2d$ positions in space group $P\bar{3}m1$. In order to calculate the electronic structure of NaLiCdS$_2$ it was necessary to place the Li atom at position $1b$ (1/3,2/3,z) and the Cd atom at position $1c$ (2/3,1/3, 1−z) in space group $P3m1$. The FP-LAPW method [19,20], as implemented in the WIEN2k code [21], was used for these calculations. Included were local orbits for high-lying semicore states. The exchange-correlations were treated in the generalized gradient approximation within density-functional theory by para-

meterization [22]. The muffin-tin radii were 2.8, 2.5, 2.53, and 2.2 Bohr for Na, Li, Cd, and S, respectively. The plane-wave expansion cutoffs for wave functions (K_{max}) and for the densities and potentials (G_{max}) were chosen as 8 and 14 Bohr^{-1}, respectively. Brillouin-zone integrations with self-consistency cycles were performed by means of a tetrahedron method [23] with the use of 800 k points throughout the Brillouin zone. For the calculation of the optical properties, 3000 k points throughout the Brillouin zone were used. The high-symmetry points are G (0, 0, 0), K (−1/3, 2/3, 0), M (0, 1/2, 0), A (0, 0, 1/2), L (0, 1/2, 1/2), and H (−1/3, 2/3, 1/2) in terms of the reciprocal basis vectors [24]. The dielectric function ε was also calculated to evaluate the optical absorption.

3. Results and discussion

3.1. Syntheses and structure

The compounds NaLiCdS$_2$ and NaLiZnS$_2$ have been synthesized in a mixed Na$_2$S/S/Li$_2$S flux at 773 K. The yields are about 80% for NaLiCdS$_2$ and 50% for NaLiZnS$_2$.

These two compounds are isostructural. The Li and (M = Cd or Zn) atoms are disordered. The compounds possess the Ce$_2$O$_2$S structure type [25], with M/Li in the Ce positions, S in the O positions, and Na in the S position. The structure of NaLiMS$_2$ is shown in Fig. 2. It consists of two-dimensional $^2_\infty$[LiMS$_2$] layers stacked perpendicular to the [001] direction. The two-dimensional layers, which are ruffled, are formed by corner-sharing LiS$_4$ tetrahedra or MS$_4$ tetrahedra, as indicated in Fig. 3. The layers are separated by Na atoms (site symmetry $\bar{3}m$) that are surrounded by six S atoms, three from each layer. The Li or M atoms, which have site symmetry $3m$, are coordinated to one axial and three equatorial S atoms. The interatomic distances in these compounds are reasonable when compared to those in structures in which the given atoms have similar coordination geometries. For example, the Na–S distances for NaLiZnS$_2$ and NaLiCdS$_2$ of 2.9100(5)
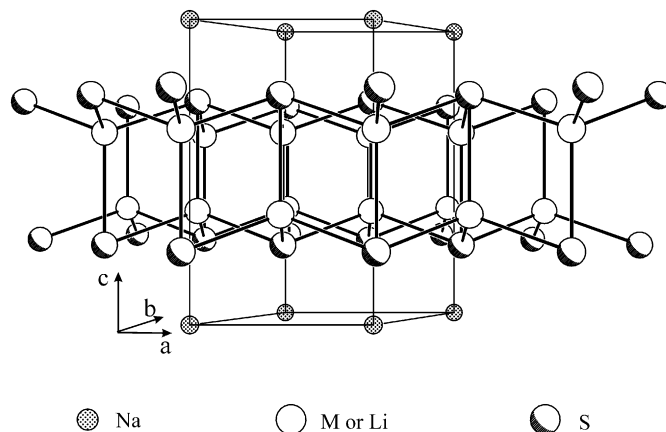

Fig. 2. Crystal structure of NaLiMS$_2$ (M = Cd, Zn).
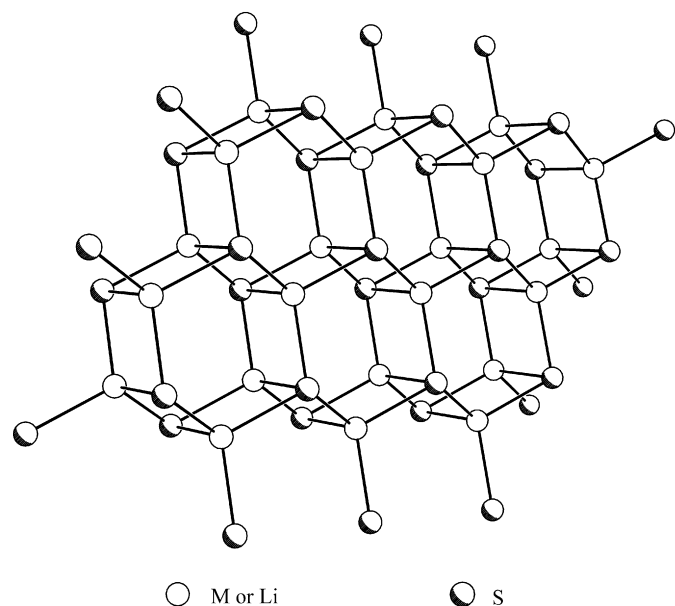
Fig. 3. The structure of the two-dimensional $^2_\infty[LiMS_2]$ layer.

and 2.9590(3) Å, respectively, are comparable to those in Na_3TaS_4 (2.852(3) to 3.239(2) Å) [26]. The M–S distances of 2.3987(3) and 2.429(1) Å for $NaLiZnS_2$ and 2.5039(2) and 2.6051(7) Å for $NaLiCdS_2$ may be compared to those of 2.416(4) Å for Zn–S or Li–S in $KLiZnS_2$ [15], 2.473(2) to 2.671(3) Å for Cd–S in $K_2Cd_3S_4$ [27], and 2.52(2) to 2.53(1) Å for Li–S in LiAuS [3].

3.2. Absorbance spectrum

The absorbance spectrum obtained with polarized light perpendicular to the (0 0 1) crystal face of a single crystal of $NaLiCdS_2$ is shown in Fig. 4a. Electronic structure calculations indicate that $NaLiCdS_2$ is semiconducting (see below). In order to determine the nature of the transition at about 2.4 eV the scaled absorption value and the crystal thickness were used to calculate the absorption coefficient α [28]. Plots of $(\alpha h\nu)^2$ vs. $h\nu$ (Fig. 4b) and $(\alpha h\nu)^{1/2}$ vs. $h\nu$ (Fig. 4c) show that the optical transition is indirect [29,30]. The optical transition was determined to be indirect because the fit in Fig. 4b is superior to that in Fig. 4c. The intersection of the least-squares lines of baseline and band edge [28] lead to an optical band gap of 2.37 eV. This value is consistent with the reddish-yellow color of the compound and agrees well with theory.

3.3. Electronic structure

The total and partial density of states (DOS) of $NaLiCdS_2$ are shown in Fig. 5. The Na, Li, Cd, and S orbitals are highly overlapped in the valence band and the conduction band, which can be seen from the overlap among them around the Fermi level. The heavier alkali metals (Cs, Rb, K) usually make no contributions around
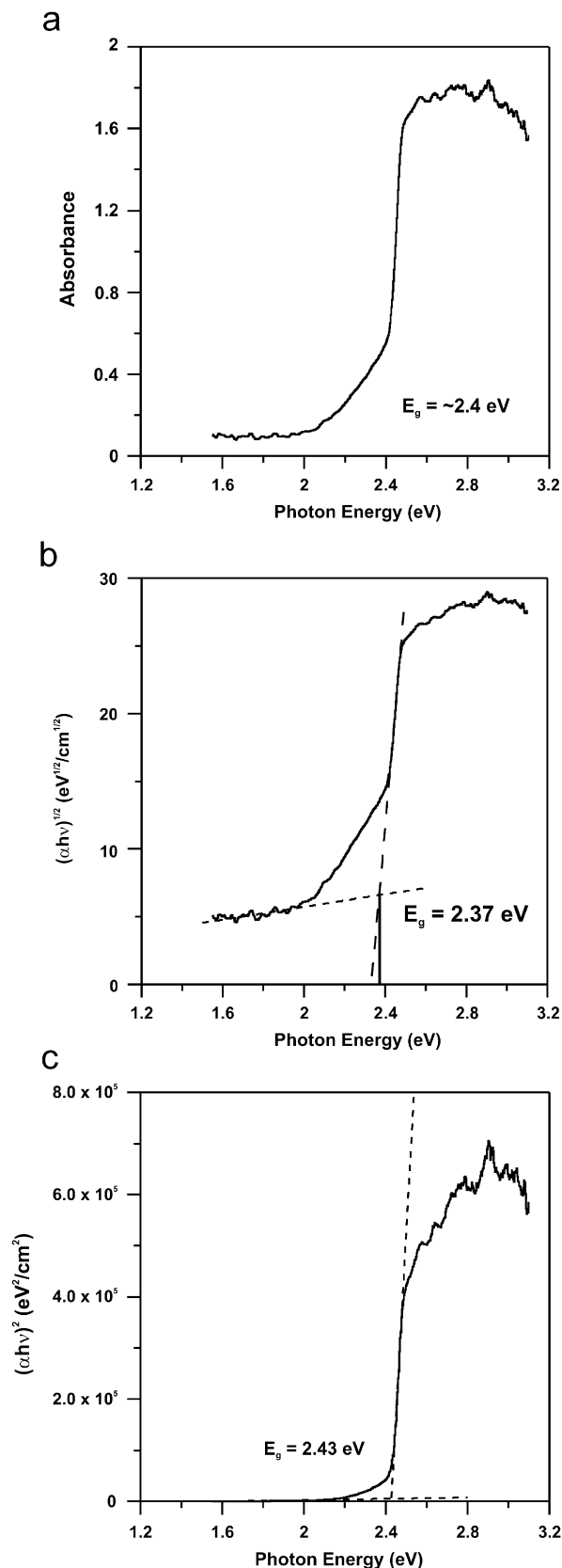

Fig. 4. (a) Absorbance spectrum of $NaLiCdS_2$; (b) plot for an indirect transition; and (c) plot for a direct transition.
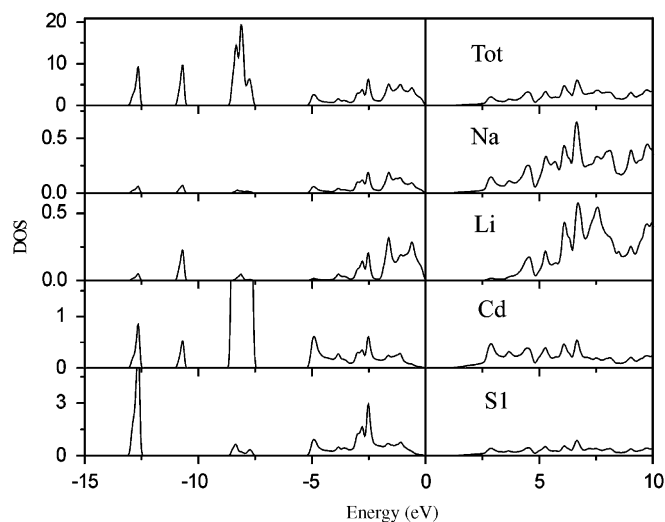
Fig. 5. Total and partial densities of states (DOS) of NaLiCdS$_2$. The Fermi level is at 0.

Fig. 6. Band structure of NaLiCdS$_2$ (dashed lines indicate the transition from $G \rightarrow A$ to $M \rightarrow G$).

the Fermi level and hence exert almost no effects on the electronic structures of comparable compounds, for example KSm$_2$CuS$_4$ [31], RbLnSe$_2$ [32], and CsLnMSe$_3$ ($M =$ Zn, Cd, Mn) [28]. However, in NaLiCdS$_2$ the contributions of the Na 3s electrons around the Fermi level, and thus to the electronic structure, cannot be ignored. These contributions are about 30% of those of the Li 2s and Cd 5s electrons. The latter contributions are mainly in the conduction band. In the region from -5 eV to the Fermi level, the Li 2s and Cd 5s electrons also contribute. The Cd 4d orbitals are highly localized, as can be seen from the sharp peak near -8 eV. Because the Li and Cd atoms are disordered in the crystal structure, the electronic structure in the region from -5 eV to the Fermi level should be the average of the contributions of Li and Cd. The S 3s electrons are highly localized and exhibit a sharp peak near -13 eV. The S 3p orbitals lie mostly in the valence band, where Na–S, Li–S, and Cd–S interactions are formed.

The smallest direct transition between the valence band and the conduction band is only about 1.0 eV (Fig. 6), which is much smaller than the measured band gap of 2.37 eV. Although the theory employed underestimates band gaps, from our experience with other metal chalcogenide systems, for example KSm$_2$CuS$_4$ [31], K$_2$CuSbS$_3$ [33], and RbLnSe$_2$ [32], the underestimation should be less than 1.0 eV. Therefore, the band structure (Fig. 6) was calculated in order to obtain additional insight into the band gap. There is only one band in the region from $+1.0$ to 4.0 eV above the Fermi level. This region consists mainly of Cd 5s orbitals. The bands below the Fermi level are mainly composed of S 3p orbitals. The smallest direct transition, about 1.0 eV, is located at the G (0,0,0) point, as shown in Fig. 6. Note that the dispersion in the Cd 5s band is very large at the G (0,0,0) point. A large dispersion (steep bands with a large slope dE/dk in a band structure)
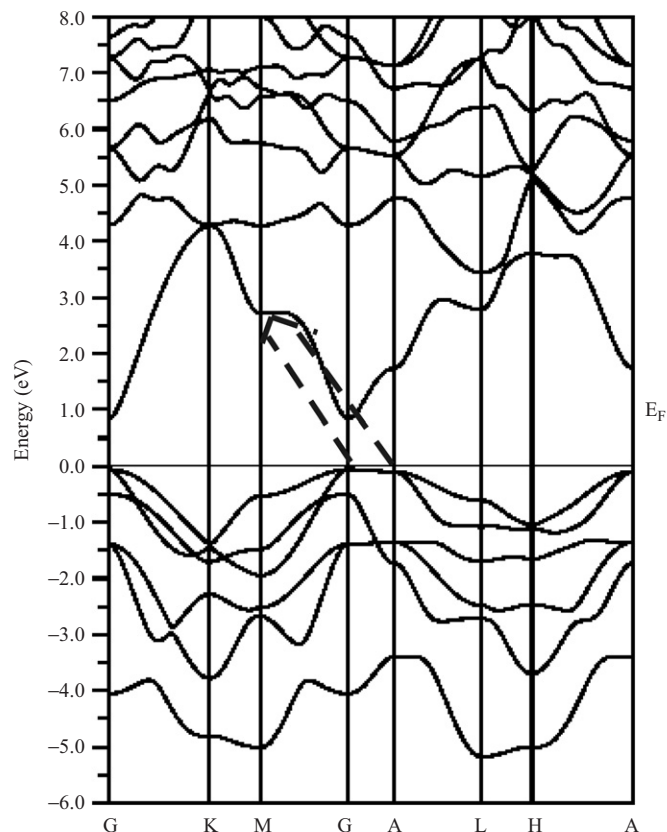
corresponds to small density states, and small dispersion (flat bands with a small slope dE/dk in the band structure) corresponds to large density states [34], which can also be seen from the comparison of Figs. 5 and 6. Therefore, there only a few states at the G(0,0,0) point and the direct transition at this point is too weak to be measured. The strong optical transitions are due to flat bands from the valence band to the conduction band. A flat curve is found along the G point to the A point in the valence band as well as along the M point to the G point in the conduction band. The transition from $G \rightarrow A$ to $M \rightarrow G$ (dashed arrows in Fig. 6) exhibits a gap of about 2.4 eV, in agreement with the experimental value of 2.37 eV. More importantly, the transition is indirect as is also deduced from the absorption data.

The dielectric function was calculated to provide more information about the optical absorption. Fig. 7 shows the imaginary component of the dielectric tensor ε^{zz}, which is directly proportional to the absorption properties of the (001) face. There is a weak optical absorption at about 1.0 eV and a strong absorption at about 2.4 eV; this confirms our assignment of the optical transition. On this basis, we conclude that the main band-gap excitations for NaLiCdS$_2$ arise primarily from S$\rightarrow$Cd charge-transfer transitions at 1.0 eV (very weak) and 2.4 eV (strong); these result in the observed red–yellow color of the material.
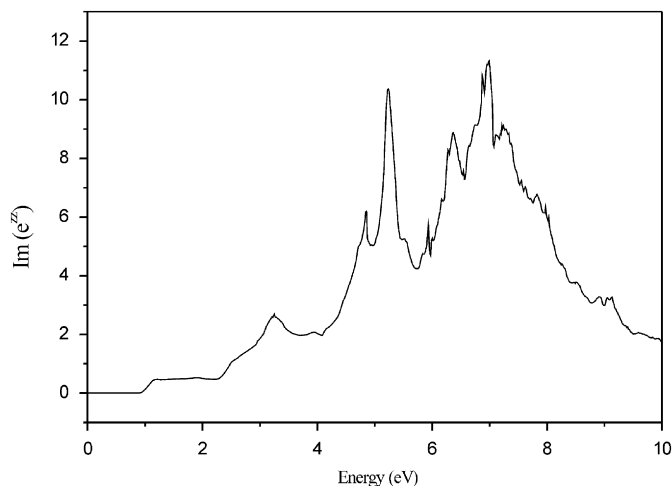
Fig. 7. The imaginary part of dielectric tensor ε^{zz}.

4. Supporting information

The crystallographic files in cif format for $NaLiCdS_2$ and $NaLiZnS_2$ have been deposited with FIZ Karlsruhe as CSD Nos. 417089 and 417088, respectively. These data may be obtained free of charge by contacting FIZ Karlsruhe at +49 7247 808 666 (fax) or crysdata@fix-karlsruhe.de (e-mail).

Acknowledgments

References

[1] M.G. Kanatzidis, A.C. Sutorik, Prog. Inorg. Chem. 43 (1995) 151–265.
[2] S.A. Sunshine, D. Kang, J.A. Ibers, J. Am. Chem. Soc. 109 (1987) 6202–6204.
[3] F.Q. Huang, Y. Yang, C. Flaschenriem, J.A. Ibers, Inorg. Chem. 40 (2001) 1397–1398.
[4] Y. Matsushita, M.G. Kanatzidis, Z. Naturforsch. B: Chem. Sci. 53 (1998) 23–30.
[5] J.A. Aitken, G.A. Marking, M. Evain, L. Iordanidis, M.G. Kanatzidis, J. Solid State Chem. 153 (2000) 158–169.
[6] J.A. Aitken, K. Chondroudis, V.G. Young Jr., M.G. Kanatzidis, Inorg. Chem. 39 (2000) 1525–1533.
[7] J.A. Aitken, P. Larson, S.D. Mahanti, M.G. Kanatzidis, Chem. Mater. 13 (2001) 4714–4721.
[8] G.A. Marking, M.G. Kanatzidis, J. Alloys Compds. 259 (1997) 122–128.
[9] J.A. Aitken, M.G. Kanatzidis, Inorg. Chem. 40 (2001) 2938–2939.
[10] F.Q. Huang, B. Deng, J.A. Ibers, J. Solid State Chem. 178 (2005) 194–199.
[11] Bruker, SMART Version 5.054 Data Collection and SAINT-Plus Version 6.45a Data Processing Software for the SMART System, Bruker Analytical X-ray Instruments, Inc., Madison, WI, USA, 2003.
[12] G.M. Sheldrick, SHELXTL Version 6.14, Bruker Analytical X-ray Instruments, Inc., Madison, WI, USA, 2003.
[13] H. Sabrowsky, A. Thimm, P. Mertens, Z. Naturforsch. B: Anorg. Chem. Org. Chem. 40 (1985) 733–735.
[14] H. Sabrowsky, K. Hippler, R.-D. Hitzbleck, S. Sitta, A. Thimm, P. Vogt, R. Wortmann, Z. Naturforsch. B: Chem. Sci. 44 (1989) 893–895.
[15] D. Schmitz, W. Bronger, Z. Anorg. Allg. Chem. 553 (1987) 248–260.
[16] J. Leal-Gonzalez, S.S. Melibary, A.J. Smith, Acta Crystallogr. Sect. C: Cryst. Struct. Commun. 46 (1990) 2017–2019.
[17] R.D. Shannon, Acta Crystallogr. Sect. A: Cryst. Phys. Diffr. Theor. Gen. Crystallogr. 32 (1976) 751–767.
[18] L.M. Gelato, E. Parthé, J. Appl. Crystallogr. 20 (1987) 139–143.
[19] E. Wimmer, H. Krakauer, M. Weinert, A.J. Freeman, Phys. Rev. B 24 (1981) 864–875.
[20] M. Weinert, E. Wimmer, A.J. Freeman, Phys. Rev. B 26 (1982) 4571–4578.
[21] P. Blaha, K. Schwarz, G.K. Madsen, D. Kvasnicka, J. Luitz, WIEN2k. An Augmented Plane Wave + Local Orbitals Program for Calculating Crystal Properties, Karlheinz Schwarz, Techn. Universität Wien, Austria, Vienna, 2001.
[22] J.P. Perdew, Y. Wang, Phys. Rev. B: Condens. Matter 45 (1992) 13244–13249.
[23] P.E. Blöchl, O. Jepsen, O.K. Andersen, Phys. Rev. B: Condens. Matter 49 (1994) 16223–16233.
[24] C.J. Bradley, A.P. Cracknell, The Mathematical Theory of Symmetry in Solids. Representation Theory for Point Groups and Space Groups, Clarendon Press, Oxford, 1972.
[25] W.H. Zachariasen, Acta Crystallogr. 2 (1949) 60–62.
[26] S. Herzog, C. Näther, P. Dürichen, W. Bensch, Z. Anorg. Allg. Chem. 624 (1998) 2021–2024.
[27] E.A. Axtell III, J.-H. Liao, Z. Pikramenou, M.G. Kanatzidis, Chem. Eur. J. 2 (1996) 656–666.
[28] K. Mitchell, F.Q. Huang, A.D. McFarland, C.L. Haynes, R.C. Somers, R.P. Van Duyne, J.A. Ibers, Inorg. Chem. 42 (2003) 4109–4116.
[29] J.I. Pankove, Optical Processes in Semiconductors, Prentice-Hall, Inc., Englewood Cliffs, NJ, 1971.
[30] T.-H. Bang, S.-H. Choe, B.-N. Park, M.-S. Jin, W.-T. Kim, Semicond. Sci. Technol. 11 (1996) 1159–1162.
[31] J. Yao, B. Deng, D.E. Ellis, J.A. Ibers, J. Solid State Chem. 176 (2003) 5–12.
[32] B. Deng, D.E. Ellis, J.A. Ibers, Inorg. Chem. 41 (2002) 5716–5720.
[33] B. Deng, G.H. Chan, D.E. Ellis, R.P. Van Duyne, J.A. Ibers, J. Solid State Chem. 178 (2005) 3169–3175.
[34] R. Hoffmann, Solids and Surfaces: A Chemist's View of Bonding in Extended Structures, VCH, New York, 1988.